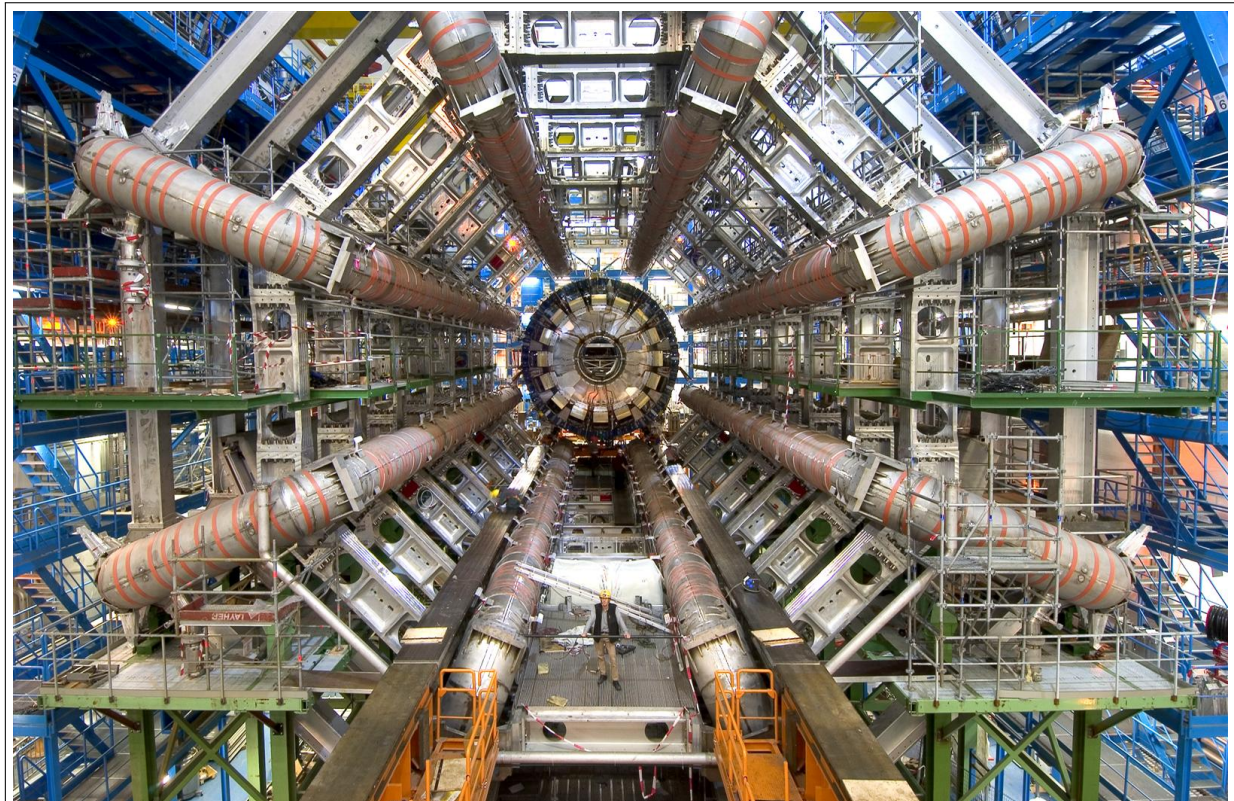


E214: ATLAS

Kanhaiya Gupta and Chelsea Maria John
Supervised by Christian Nass

Rheinische Friedrich-Wilhelms Universität Bonn.
Adavnced Lab Course

March 31, 2020



Contents

1	Introduction	2
2	Theoretical Background	2
2.1	Standard Model	2
2.1.1	Feynman Diagrams	3
3	Interactions in the Standard Model	3
3.0.1	Electromagnetic Interactions	3
3.0.2	Strong Interactions	4
3.0.3	Weak Interactions	4
3.0.4	Electroweak Interaction	5
4	The Search Of New Physics	5
4.1	Higgs Mechanism	5
4.2	SuperSymmetry	5
4.3	SUSY in ZZ^* spectrum	6
4.4	Fourth Generation Quarks	6
4.5	Additional gauge bosons	6
5	Particle Detection	6
5.1	The Large Hadron Collider(LHC)	7
5.2	The ATLAS Detector	7
5.2.1	The Inner detector	7
5.2.2	Solenoid	8
5.2.3	The Presampler	8
5.2.4	Electromagnetic Calorimeter (ECAL)	8
5.2.5	Hadronic Calorimeter (HCAL)	8
5.2.6	Muon Spectrometer	8
6	Event Kinematics	9
7	Experiment	9
7.1	Part 1: Graphic Display of Particle Reactions	9
7.2	Assignment 1	9
7.3	Assignment 2	10
7.3.1	Task 3	10
7.3.2	Task 5	11
7.4	Part 2 : Calibration of Electrons	11
7.4.1	Assignment 3	11
7.4.2	Assignment 4	12
7.5	Discussion	12
8	BEYOND THE STANDARD MODEL:ANALYSIS OF Z^0Z^0 PAIR DECAY	13
8.1	Identifying the Z^0Z^0 Pair	13
8.2	The three types of decay: ZZ, ZZ^* and Z^*Z^*	15
8.3	New Physics	15
8.4	Higgs' Mechanism	16
8.5	Heavy Gauge Bosons Z^0	16
8.6	Supersymmetry Model	17
8.7	Fourth Generation quarks	18
9	Conclusion	18
10	Acknowledgement	19
11	Appendix	20

1 Introduction

The Large Hadron Collider (LHC) at CERN and its experiments were conceived to tackle open questions in particle physics. The mechanism of the generation of mass of fundamental particles has been elucidated with the discovery of the Higgs boson. The standard model of particle physics is a remarkable theory in providing that provides the explanation of the particles physics and their interactions. Yet, it fails to explain the matter-antimatter asymmetry that exist in the universe, the dark matter, dark energy etc.

In this laboratory experiment[1], we analyse the simulated data for the search of Higgs boson and beyond standard model of particle physics called as new physics using the event display software ATLANTIS and the high energy physics data analysis software ROOT.

2 Theoretical Background

2.1 Standard Model

The Standard model is used to describe the interactions of fundamental particles in particle physics by means of quantum field theories that are based on the principle of local gauge invariance. The fundamental particles are divided based on their spins into fermions (half-integer spins) and bosons (integer spins). The fermions (quarks, leptons and neutrinos) are building blocks of matters while bosons are mediators of the three fundamental interactions – Electromagnetic (via photons), Strong (via gluons) and Weak (charged current via W^\pm and neutral current via Z^0). The quarks and leptons have three generations where the generations increase in mass and higher generations decay into lower generation particles. Furthermore, each particle has a corresponding anti-particle with opposite charges. Gravity despite being a fundamental force is too weak to play any significant role in particle physics scale. The Standard model also includes the Higgs boson, which is used to give mass to elementary particles.

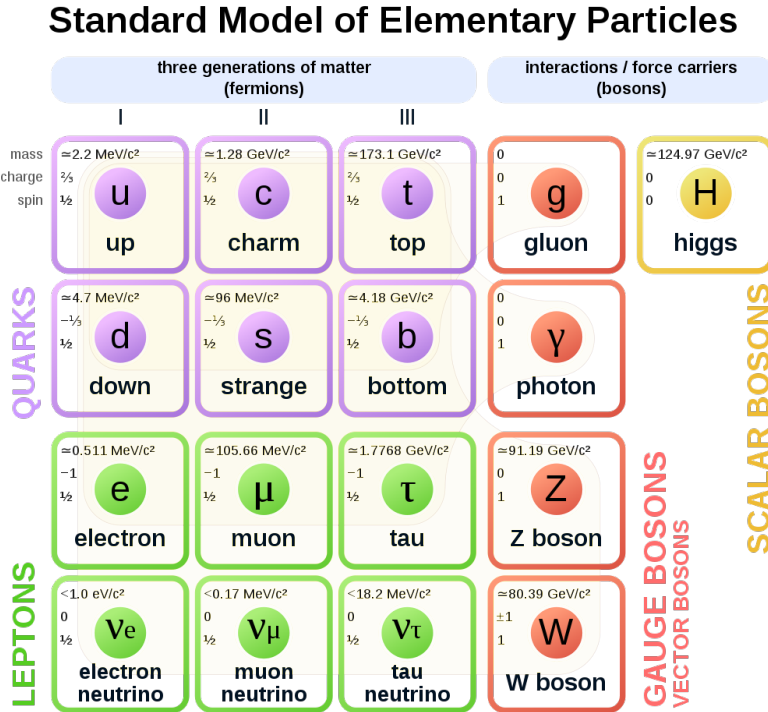


Figure 1: Standard Model[2]

2.1.1 Feynman Diagrams

Feynman diagrams are schematic representations of particle interactions that are used to make calculations like cross sections of particles easier. The diagrams are drawn based on certain rules called Feynman rules which comply with the conservation laws. The external lines in the diagram represent initial and final physical states of particle, thereby abide by the Energy-Momentum relation or are "on mass shell". The internal lines represents virtual particles that do not obey the Energy-Momentum relation or are "off shell" and exists only within the limits of uncertainty relation. Each vertex is associated with a coupling factor that describes the interaction strength and depending on the order of the diagram, it can contain a number of loops.

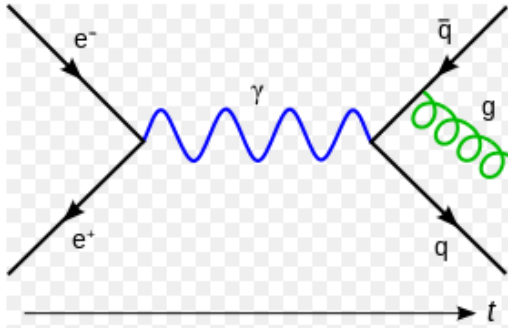


Figure 2: Feynman Diagram of a real radiative correction in QCD[3]

3 Interactions in the Standard Model

Apart from gravitational interactions, which are still described classically. The other three interactions are currently explained quantum mechanically in the Standard Model. A brief description of each theory is mentioned below.

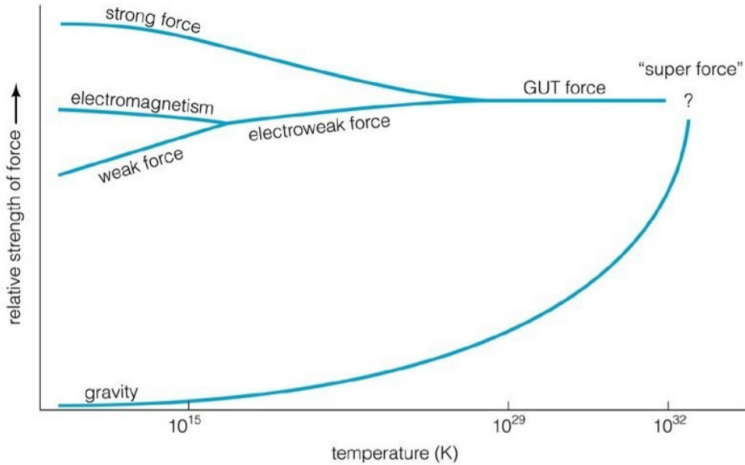


Figure 3: Running Couplings behavior with increasing energies hypothesizing the existence of a grand unified theory(GUT) and a theory of everything(TOE)[4].

3.0.1 Electromagnetic Interactions

Electromagnetic interaction is described using the theory of Quantum Electrodynamics (QED) which is a perturbation theory combining Special Relativity and Quantum Theory. The interactions between particles are explained via the exchange of photons using gauge theory in U(1) symmetry. The electromagnetic

coupling constant at low momenta (Q^2) is given by the fine structure constant $\alpha_{em} = \frac{1}{137}$ and it increases with increasing Q^2 .

3.0.2 Strong Interactions

Strong interaction is described using Quantum Chromodynamics(QCD) which is defined under the SU(3) symmetry. The interactions among colour-charged particles, i.e, quarks and gluons that can carry color degrees of freedom (Red, Green, Blue) are mediated through gluons. In strong interaction, the coupling constant $\alpha_s(Q^2)$ decreases with increasing Q^2 and finally approaches zero as Q^2 goes to infinity. This phenomenon is called asymptotic freedom. At high momentum transfers the quarks within the hadron act like quasi-free particles. At low Q^2 , α_s reaches a pole and gets too large to be described by perturbative methods. A consequence of this behaviour at low momenta is the phenomenon of color confinement, that is all hadrons are colour neutral. If a highly energetic collision leads to the liberation of a bare color-charge, the highly energetic particle then creates other particles out of vacuum, forming new bound states of color-neutral non-elementary particles. In doing so, a huge amount of particles are created resulting in the formation of jets which are conical-shaped tracks pointing along the path of the original particle. Hence, color-charged particles must only exist in color-neutral states. That causes the creation of glueballs, bound states of gluons, and hadrons.

Hadrons:

The bound states of quarks and gluons are known as hadrons. There are two types: Baryons(qqq) and Mesons ($q\bar{q}$). Hadrons have sea quarks as well as valence quarks. For example in protons, (uud) are the valence quarks and the sea of various other quarks, anti-quarks and gluons are called the sea quarks. Each quark carries a fraction of the proton's momentum x and is described using the parton distribution function(PDF). Interactions between hadrons at high energies are almost always inelastic reactions in which, two partons one of each of the two hadrons interact. The reaction of the two partons is called hardscattering reaction or simply the hard event. The remaining partons move on nearly unaffected and form the rest of the event.

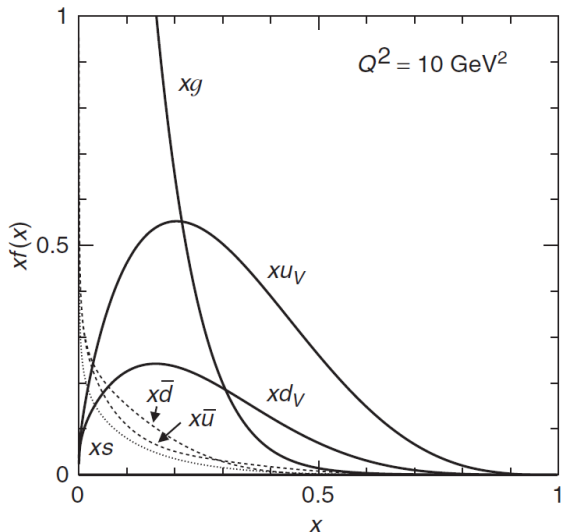


Figure 4: Graph of proton's PDF's[5]

3.0.3 Weak Interactions

The weak interaction is a gauge interaction with gauge bosons which have spin 1 and the gauge group SU(2). The weak interaction can couple quarks of different generations and hence change quarks' flavours. The interactions occur via the exchange of massive W^\pm and Z^0 bosons, where $M_{W^\pm} = 80.403 \pm 0.029$ GeV and $M_{Z^0} = 91.1876 \pm 0.0021$ GeV. Since the bosons have huge mass the interaction is very short-ranged and the fact that the mediators are massive cannot be explained by this theory alone. This led to theory of Electroweak which combines QED and weak interactions under $SU(2) \times U(1)_Y$ symmetry.

3.0.4 Electroweak Interaction

The Electroweak theory combines the electromagnetic and weak theory under $SU(2) \times U(1)_Y$ symmetry, generating four massless bosons (W_1, W_2, W_3, B), which then acquire mass via the Higgs mechanism. The bosons are then obtained by the spontaneous breaking of the $SU(2) \times U(1)$ symmetry by the Higgs mechanism, where W^\pm are linear combinations of W_1, W_2 , and Z^0, γ are a rotation of the W_3 -B plane. The angle of rotation is given by the Weinberg weak mixing angle θ_W where $\cos \theta_W = \frac{M_W}{M_Z}$.

4 The Search Of New Physics

The lab assignment places us in a scenario back to the start of LHC (2010-2011), before the Higgs was discovered. Within this scenario, we search for new physics which also includes searches for a Higgs boson.

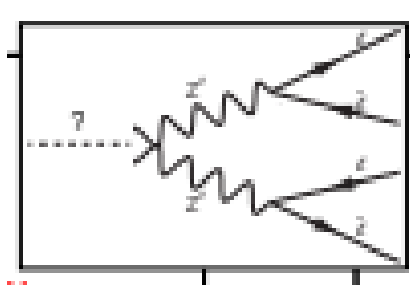


Figure 5: Higgs decay to four leptons[6]

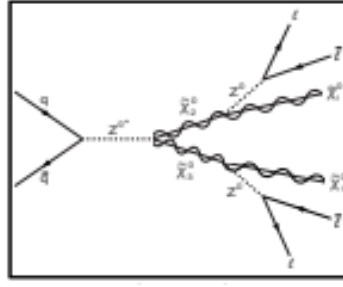


Figure 6: Susy decay cascade to four leptons[6]

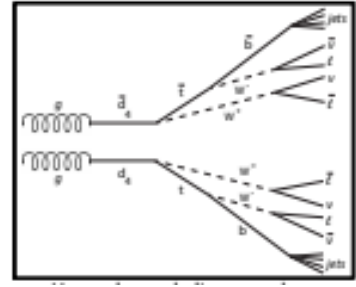


Figure 7: Heavy quark decay to four leptons[6]

4.1 Higgs Mechanism

The Higgs mechanism starts at hypothesizing a symmetry breaking by the existence of a non-zero value of the Vacuum Expectation Value VEV(246GeV), where we would have a doublet of complex scalar Higgs field whose excitation results in the Higgs boson. Then coupling of elementary particles with this field is the mechanism by which they acquire mass. Furthermore, it can be shown that a part of the EW gauge group, the electromagnetic gauge group, is unbroken. That explains why the photon is a massless boson. Furthermore, the mass of the Higgs boson is itself a free parameter of the theory. However, once fixed, all other properties of the boson can be calculated.

4.2 SuperSymmetry

Supersymmetry or SUSY is a proposed symmetry between fermions of half integer spin, and bosons of integer spin. It states that for every particle there exist superpartners that differ by a half-integer spin. There are more than one SUSY candidates, the one proposing the least number of superpartners is the Minimal Supersymmetric Standard Model (MSSM) in which there is exactly one superpartner for each particle.

The SUSY theory offers solutions to the following problems in Standard Model:

- 1) According to the theory of GUT¹, there should be an energy scale where all the coupling constants converge and restore the hypothetical unified interaction. In Standard model the extrapolation of couplings towards high energies does not indicate that the couplings meet at one point ,but in SUSY all running couplings unite at a scale of about 10^{16} GeV.
- 2) The introduction of Superpartners of Standard model particles solves the fine-tuning problem and thus provides an accurate calculation of the Higgs mass that is consistent with the experiment.
- 3) SUSY offers a candidate for dark matter, the so called "Lightest Supersymmetric Particle" (LSP). If the LSP is electrically neutral, it will hardly interact with the visible matter.
- 4) The formulation of Supersymmetry as a local symmetry might allow an interrogation of the gravity into quantum field theory(so-called Supergravity models).

¹Grand Unified Theory

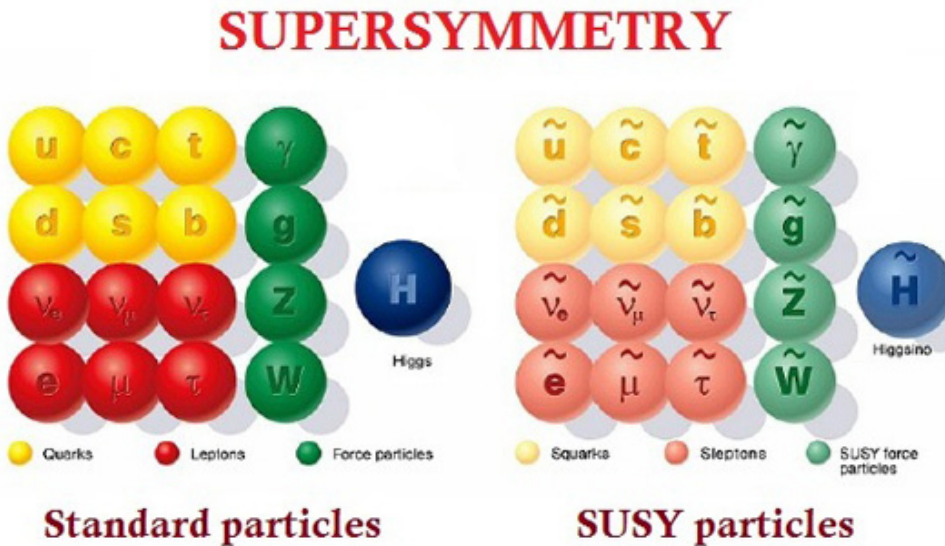


Figure 8: Supersymmetry proposes that every particle in the Standard Model, shown at left, has a “superpartner” particle[7].

4.3 SUSY in $Z Z^*$ spectrum

In the MSSM, the mixing of Higgs field and the neutral electroweak gauge bosons results in four measurable states called neutralinos. Some SUSY models predict that the lightest neutralino $\tilde{\chi}_1^0$ is the lightest SUSY particle LSP. The higher neutralinos ($\tilde{\chi}_2^0, \tilde{\chi}_3^0$) each decay to the lightest neutralino $\tilde{\chi}_1^0$ by radiating a Z^0 boson. The $\tilde{\chi}_1^0$ causes an imbalance in the observable transverse momentum, thus a considerable value of E_T .

4.4 Fourth Generation Quarks

If there are heavy neutrinos then the number of generations are not restricted to three. The corresponding quarks of the generations must be then heavier than top quark or else they would have been already detected. The decays of the hypothetical quarks of the fourth generation depends on whether it is an up-type with charge +2/3 or down-type with charge -1/3.

If the fourth generation down type quark is d_4 and up-type is u_4 , the decays occur as following:

$$gg \rightarrow d_4 \bar{d}_4 \rightarrow tW^- \bar{t}W^+ \rightarrow bW^+W^- \bar{b}W^-W^+ \quad (1)$$

$$gg \rightarrow u_4 \bar{u}_4 \rightarrow bW^- \bar{b}W^+ \quad (2)$$

4.5 Additional gauge bosons

The theories sometimes predict the existence of additional heavy gauge bosons (Z' and W') with properties similar to the Z^0 boson and would decay to quark or lepton pairs.

5 Particle Detection

Recent advances in our knowledge of the phenomena of high-energy physics and of the elementary particles has resulted from rapid advances in the technology of particle accelerators and the art of particle detection. The instruments for the detection of energetic particles can be divided into two classes (i) the track-imaging device in which one sees or photographs tracks which coincide with the actual path taken by the particle and (ii) counting devices which gives only an indication that particles pass somewhere in the sensitive volume. Here, we discuss about the proton-proton accelerator at CERN called the Large Hadron Collider and the ATLAS detector which is based on image-tracking.

5.1 The Large Hadron Collider(LHC)

The Large Hadron Collider (LHC) is a circular proton-proton accelerator which was built at the European Center for Particle Physics(CERN) Geneva, Switzerland . The LHC is installed in the old tunnel of the LEP accelerator which is buried about 100 meters below the ground near Geneva. It consists of a 27 km ring of a superconducting magnet along with accelerating structures. Inside the ring, two highly energetic beams of particles travel in opposite directions, in separate pipes, at speeds very close to the speed of light. The beams are guided through that circular path by numerous installed magnet structures; 1232 dipole magnets each of length 14 m for bending the particle beams, 392 quadrupole magnets each of length 5 to 7 m for focusing of the beams. The LHC collides proton-proton, proton-ion, or ion-ion beams. This experiment however is based on data collected from proton-proton collisions. Protons originate from a hydrogen source and are accelerated to an energy of 7.0 TeV. They are then brought to a head-on collision which results in the production of many subatomic particles. In order to collect data from the LHC collisions, four crossing points are present, around which 7 detectors are placed, namely; ATLAS, CMS,LHCb, ALICE, TOTEM, LHCf, and MoEDAL. This experiment uses data collected by the ATLAS detector.

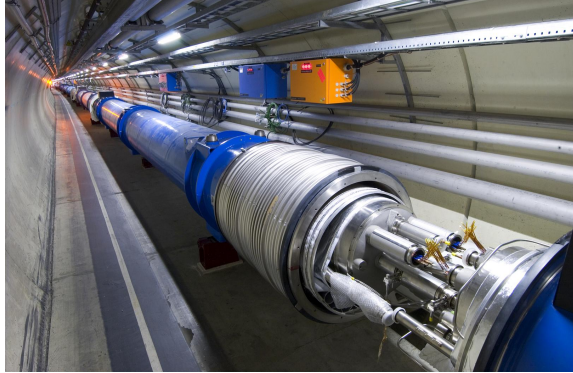


Figure 9: Part of LHC ring[8]

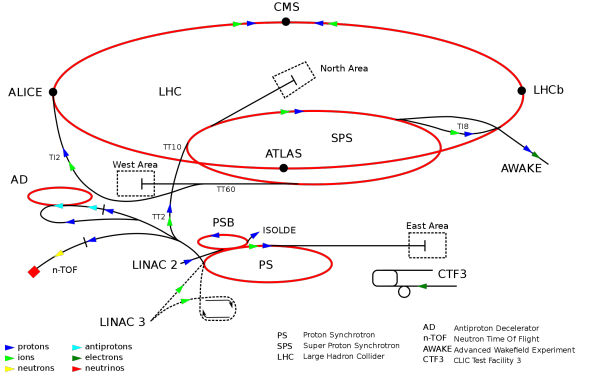


Figure 10: CERN Accelerator Complex[9]

5.2 The ATLAS Detector

The A Toroidal LHC Apparatus (ATLAS) is a cylindrical detector with a length of 46m and a height of 25m. Looking from the centre of the detector to the outside the folowing components helps in particle identifications and Energy-Momentum calculations :

5.2.1 The Inner detector

The Inner detector is used to measure the momentum ,charge and direction of charged partciles produced in a applied magnetic field. It consists of three parts:

- Pixel Detector: It is a silicon pixel detector locted at the innermost part of the detector at a radial distance of 5cm to 15cm from the beam pipe. It is used to measure the trajectories very precisely and reconstruct the primary interaction point as well as the secondary vertices which can occur in the decay of long-living hadrons containing b-quarks.
- The Semi-Conductor Tracker(SCT): It consists of silicon microstrip sensors and is part of the tracking system.
- The Transition Radiation Detector(TRT): It is the outer most component of the inner detector. It consists of drift chambers filled with gas currently- $Xe(70\%)CO_2(27\%)O_2(3\%)$. The signal generated by the ionizing particles is further enhanced by transistion radiation produced by alternate layers of materials with different refractive index. It helps in the identification of electrons.

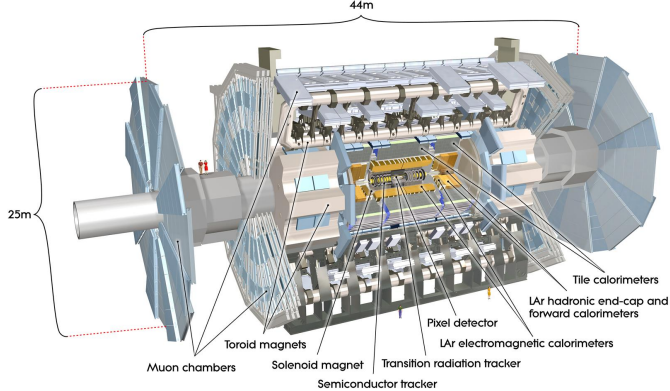


Figure 11: Computer Generated image of ATLAS detector[10]

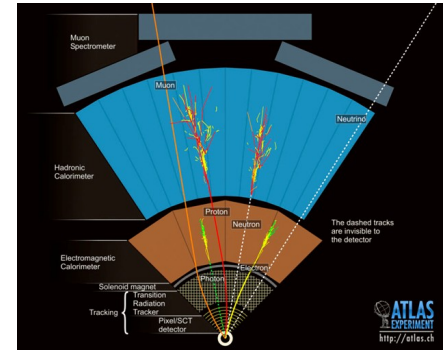


Figure 12: Graphical representation of tracks of different particles detected by ATLAS[11]

5.2.2 Solenoid

The solenoid provides magnetic field in the direction parallel to the beam axis for the inner detector ($B = 2$ Tesla).

5.2.3 The Presampler

It supports the electromagnetic calorimeter in measuring the electromagnetic showers and distinguishing single photons and photon pairs from π^0 decays.

5.2.4 Electromagnetic Calorimeter (ECAL)

The ATLAS ECAL design consists of accordion-shaped lead and steel plates ,to allow particles to cross large amount of matter. It measures the enegry of partciles that interact electromagnetically. When a highly energetic particle, like an electron passes through, it interacts with the plates producing a large shower of electrons, positrons and photons until it eventually stops. The negative charges are attracted to the copper grid where the measured charge is used to determine the energy of the original particle.

5.2.5 Hadronic Calorimeter (HCAL)

It is used to detect the energy deposited by hadrons. It is made from alternating sheets of iron and scintillator material. A higly energetic particle creates a cascade of showers on intercating with the material and hit the scintillator tiles radiating light whose intensity is used to calculate the particles initial energy. Since the hadronic interaction length is greater than the Electromagnetic one, the HCAL has to be much deeper and denser than the ECAL.

5.2.6 Muon Spectrometer

Starting at a radius of 4.25m filling the rest of the detector till 11m is the muon spectrometer. Very few particles other than muons can pass through all inner parts reaching the spectrometer. Furthermore, a magnetic field provided by 3 toroidal magnets as well as a design of gas-filled straw tubes allows for accurate measurement of muons' momenta. The spectrometer functions in a similar fashion to that of the inner detector.

The neutrinos pass undetected through the detector and are detected using indirect methods such as calculating the missing transverse momentum.

6 Event Kinematics

1)The correlation of the invariant mass of the hard system x_A and x_B is given by :

$$\hat{s} = p_{Hard}^2 = sx_Ax_B \quad (3)$$

where \sqrt{s} is the centre of mass energy and p_{Hard} the momentum of hard event.

2) In systems where the invariant mass is zero, pseudo rapidity η which depends only on polar angle θ is defined as :

$$\eta = -\ln \tan(\theta/2) \quad (4)$$

In ATLAS, leptons can be detected in the angular range of $-2.5 < \eta < +2.5$ and jets in the range $-5 < \eta < +5$.The angular distributions of final state hadrons increases strongly in the forward direction.Particle frequencies plotted versus η are usually gaussian, sometimes with a flat plateau in the central region around $\eta = 0$

3) In hadron collisions most of the energy vanishes undetected along the beam pipe.Thus a more convenient quantity is the transverse energy of the particle $E_T = E \cdot \sin \theta$ and the total transverse energy of the event $\Sigma_i E_T = \Sigma E_i \cdot \sin \theta_i$, where E_i is the i-th energy entry in the calorimeter and θ_i is the polar angle of the entry.The total transversal energy is a useful measurement of the hardness of a hadron collision and it's values lies in the range of some 10 GeV to several TeV for hard events.

4)If there is exactly one particle like neutrinos that leaves the detector without being detected in the event, then the tranverse momentum of that neutrino can be measured as follows:

$$\vec{p}_T(\text{neutrino}) = -\sum_i \vec{p}_{T(i)} \quad (5)$$

where $\vec{p}_{T(i)} = E_i \cdot \sin \theta_i \vec{n}_{i,\perp}$ and $\vec{n}_{i,\perp}$ denotes the unit vector pointing towards the energy entry in the x-y plane. This quantity is called the missing transverse momentum \cancel{E}_T ,

$$\cancel{E}_T = -\sum_i E_i \cdot \sin \theta_i \vec{n}_{i,\perp} \quad (6)$$

This equation utilizes the total momentum balance of the event in the plane perpendicular to the beams.

In the events with several weakly interacting particles the value of \cancel{E}_T depends on the relative orientation of the direction of the undetected particle. For an example, in an event with two neutrinos which have exactly opposite transverse momenta, the observed \cancel{E}_T is zero, although a lot of energy leaves the detector without being measured. This is the main reason why calorimeters are built to cover the full solid angle and gaps in the detector can also lead to false measurements of E_T .

Considering the W^\pm and Z^0 bosons production up to the lowest order, then they have effectively no transverse momenta. However, when taking higher order interactions into account in which other partons are produced in the form of jets, then there is a net recoil of the produced bosons, hence, a net despite being small transverse momentum.

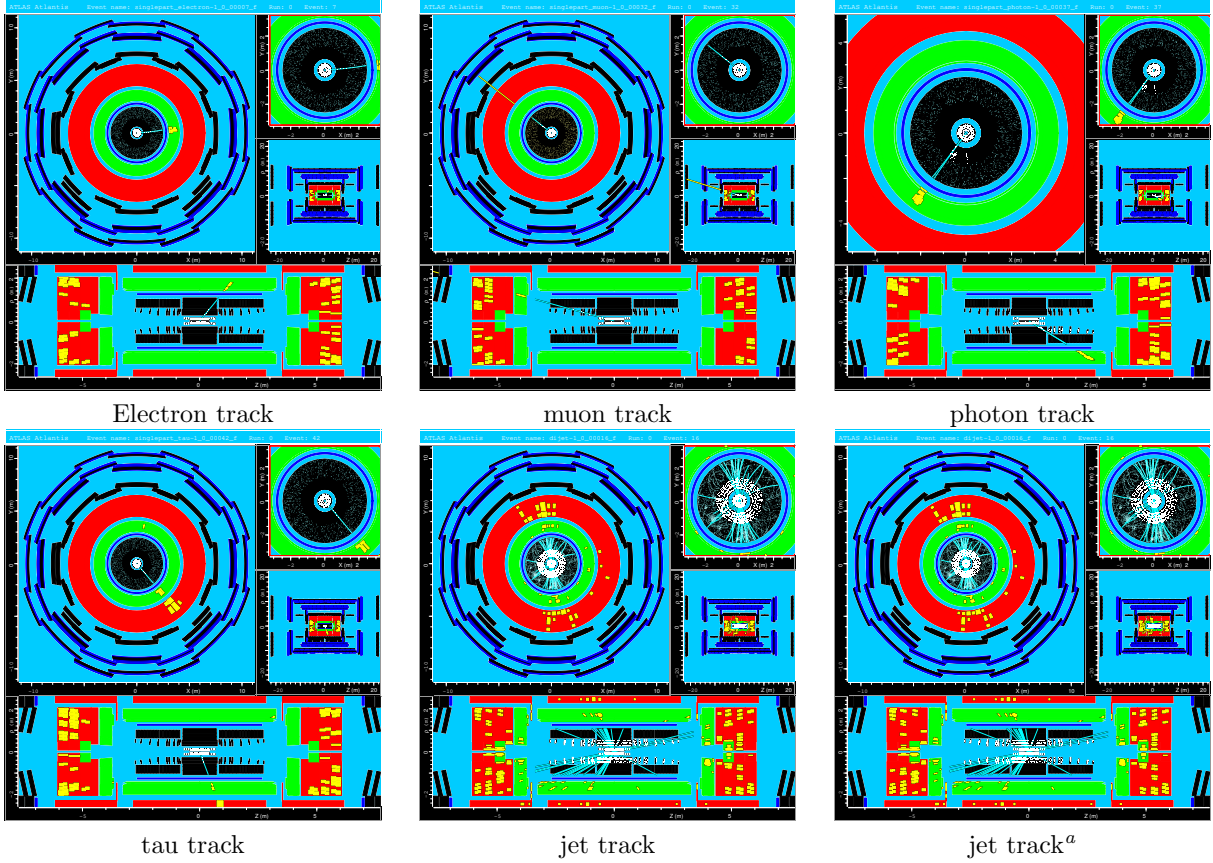
7 Experiment

7.1 Part 1: Graphic Display of Particle Reactions

In this section of the experiment, we familiarize ourselves with the ATLANTIS software which is an event display for the ATLAS experiment at CERN's Large Hadron Collider. It is written entirely in Java and used for visual investigation and the understanding of the physics of complete events. In order to get familiarize ourself we first load event data files (learning data sets) of electrons, muons, photons, tau-leptons and jets and look at various event displays. We then analyse the events and carry out two tasks based on it.

7.2 Assignment 1

The aim of this part is to get familiar with the data taking in the ATLAS experiment. This part uses ATLANTIS software for analyzing ATLAS data under different aspects. In the program ATLANTIS, the ATLAS detector's geometry, and each event are visualized where we see the tracks of the charged particle and the clusters in the calorimeters (Electromagnetic and Hadron Calorimeters). Moreover, we can also get an information about the total energy, space momentum and the missing transverse energy of the produced particle by selecting the tracks and the clusters in the ATLANTIS software. The Figure 13 shows the



^aTwo same jet tracks are shown to look the figures good.

Figure 13: Part I: Atlantis events display for the corresponding particles.

five different events (electrons, muons, photons, tau-leptons and hadronic dijets), which are visualized by ATLANTIS using learning datasets. In the pictures each region has its own color. The black region represents the inner tracking detector system which consists of the pixel detector, semiconductor tracker, and transition radiation tracker. The green color represents the electromagnetic calorimeter. The red color represents the hadron calorimeter. The outer black layers represent the muon spectrometer. The track is shown as a blue line in the inner tracking system, and we can obtain the value of the particle momentum by selecting it. The yellow colored region in the Electromagnetic and hadron calorimeters represents the electromagnetic showers and hadronic showers respectively, these regions are called clusters. We can get the information about energy loss of the particle by selecting it.

7.3 Assignment 2

After getting familiarize with the ATLANTIS software, we were suppose to carry out two tasks from the given list. We have performed the following tasks:

7.3.1 Task 3

We have loaded the muons events for this task from the muons-learning data in the ATLANTIS software. Then, we have analyzed the first twenty muon events. By clicking on the tracks in the inner detector and selecting the yellow clusters in the Electromagnetic Calorimeter, the momentum and energy of the muons can be read out. In some of the events, we observed that the momentum increased as the muon passes through the detector. This is contradictory since we know that particles lose momentum energy as they travel through a substance. Therefore, these events were not considered. Also, in one event, energy deposition in both, HCAL and ECAL was observed. The observation data has been shown in the Table 1. Average energy deposited

by Muons in the HCAL has been observed as 8.52 GeV with $\sigma = 9.11$ GeV calculated as $\sigma = \sqrt{\sum \frac{(X_i - \bar{X})^2}{N-1}}$ where \bar{X} is the mean.

Table 1: Energy, Momentum for muons

Event	Momentum P_{inn} (GeV)	Momentum P_{out} (GeV)	ΔE (GeV)
1	237.3	240.68	3.38
2	-85.28	-53.92	31.36
3	43.4	43.83	0.43
4	-241.37	-237.02	4.35
5	48.89	44.77	4.12
6	-168.16	-177.62	9.46
7	117.32	96.56	20.76
8	-71.94	-64.96	6.98
9	199.91	199.44	0.47
10	-57.84	-50.01	7.83
11	-100.75	-94.11	6.64
12	38.96	34.48	4.48
13	-105.19	-108.68	3.49
14	236.12	236.61	27.49
15	-131.69	-125.51	6.18
16	152.24	157.69	5.45
17	-35.23	-32.18	3.05
18	54.19	50.00	4.19
19	-84.75	-68.09	16.66
20	104.26	107.96	3.72

7.3.2 Task 5

In this task, we were assigned to calculate the average number of additional jets in events, in which a W boson is produced. Here, we loaded the W boson events and based on the tracks, we determined the additional jets which is shown in the Table 2. The average number of additional jets in events, in which a W boson is produced is 1, with $\sigma = 0.4$ calculated as in task 3.

7.4 Part 2 : Calibration of Electrons

In this part, calibration of electrons is done. We use the program ROOT to improve the quality of the given data so that we can reach accurate values for the W boson mass that will be measured in the next part. This calibration is important because the measured values of energies are usually not precisely correct. This can happen due to various reasons like asymmetry of the detector, inactive regions in the detector, energy losses before entry into the calorimeters and the fact that the different components vary in their efficiencies and energy yields. Consequently, the measured values are generally lower than the real values. The calibration is done in such a way that the measured invariant mass of the Z boson (from the $Z^0 \rightarrow e^+e^-$ decay) is as close as possible to the literature value.

7.4.1 Assignment 3

For this part, electron-positron pairs are investigated. Data from the electron- positron pairs form the basis of the calibration process since most of the electron-positron pairs originate from Z^0 decay. The mass of Z^0 and the width of the Z^0 signal have been measured very precisely (at the LEP Collider). So the signal produced by the highly energetic electrons in ATLAS can be calibrated using this very well known peak of Z^0 .

The data set is provided in the form of a ROOT tree. We obtained the plots for electron energy, positron energy and the invariant mass of the Z^0 boson. The invariant mass (uncalibrated) is shown in Figure 17. The peak is at around 85-86 GeV, which is quite far from the actual theoretical value.

Table 2: Average number of additional jets in which W boson is produced

Event	Invariant Mass (GeV)	Number of W bosons	Number of extra jets
1	49.10	0	0
2	89.55	1	0
3	61.88	0	0
4	104.08	1	1
5	63.73	0	2
6	66.24	0	1
7	57.57	0	2
8	197.03	2	1
9	17.77	0	0
10	85.53	1	1
11	50.95	0	2
12	146.02	1	1
13	19.53	0	0
14	137.08	1	1
15	30.50	0	0
16	21.69	0	0
17	41.16	0	1
18	93.07	0	1
19	74.86	0	1
20	46.74	0	1
21	142.00	1	1

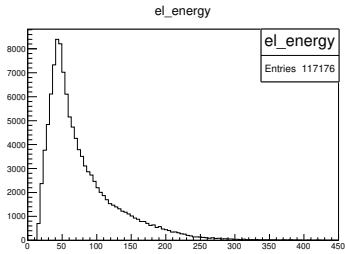


Figure 14: Electron energy

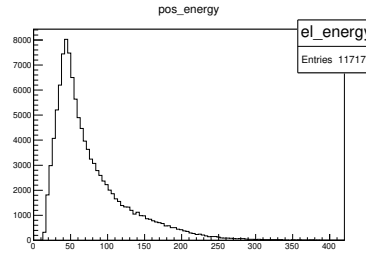


Figure 15: Positron energy

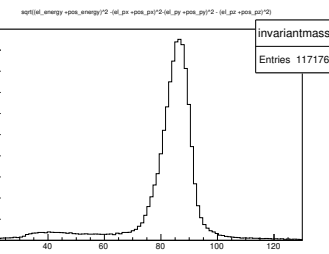


Figure 16: Invariant mass

7.4.2 Assignment 4

To get a precise value of Z^0 mass and to enhance the resolution, the invariant mass histogram is calibrated by using pre-defined parameters. The invariant mass strongly depends on these parameters: pseudo-rapidity (η), azimuthal angle (ϕ) and the energy of the electron. The range of each parameter is defined as $|\eta| < 2.5$, $\phi < \pi$ and $100 < \text{energy} < 300$ (GeV). Lower energy ranges were not considered as it gave considerably lesser values for the Z^0 mass. The correction factor has been applied to η , ϕ and transverse momentum. We did η till third order, η till second order and transverse momentum till second order. The detector regions are divided into smaller sections and for each section, the energy value was investigated by using `z.fit(" ")` command and the corresponding correction factor applied to get the desired value of energy that is 91.14 GeV. The fit after applying all the calibration also shows a peak at 91.2 GeV which looks good which is shown in Figure 18.

7.5 Discussion

At first, we see that the electron, positron energy shows a peak around 45 GeV which does not correspond to the half the Z boson mass. The same is true for the Z boson mass which we measure at 85.92 ± 0.03 . This happens because the Z boson can be not at rest as well as due to the uncalibrated detectors. The systematic error from which we start due to uncalibrated detectors is approximately $\frac{91.2 - 85.92}{91.2} = 0.0579 = 5.79\%$. So, in order to calibrate the ECAL, we applied some calibration to the detectors within certain regions of

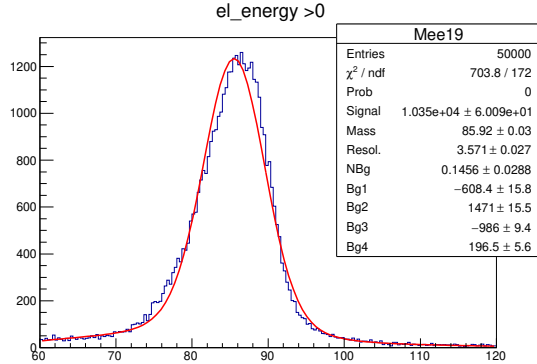


Figure 17: Invariant Mass of Z^0 (uncalibrated)

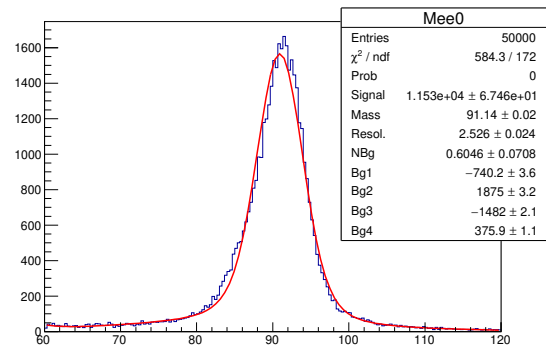


Figure 18: Calibrated electrons

pseudorapidity $\Delta\eta$. Instead of using $|\eta| < 2.5$ as a single detector, we cut it in pieces of $\Delta\eta = 0.5$ each and calibrating each of them separately moving from bigger to the smaller η 's. By doing so, the result was improved giving us a Z nominal mass value of 91.14 ± 0.02 GeV with the resolution of 2.526 ± 0.024 GeV (Figure 18). The systematic error occurring then and which we'll carry from now is decreased to approximately $\frac{91.2 - 91.14}{91.2} = 0.000657 = 0.066\%$. For a better calibration, we could have divided the detector in smaller sections by choosing smaller fractions of $\Delta\eta$ and $\Delta\phi$ '

After having calibrated the detector, we proceed further in studying the ZZ boson decays into four leptons

8 BEYOND THE STANDARD MODEL:ANALYSIS OF Z^0Z^0 PAIR DECAY

8.1 Identifying the Z^0Z^0 Pair

As mentioned before, there are other models besides the SM. One shall account here onward with four distinct cases of study, one being the Higgs Boson, another mentioned as Heavy Gauge Bosons, then SuSy that is, the Supersymmetry model, and finally the Heavy Quarks. One thus studies a similar decay process from all of the following, based on the Z^0Z^0 pair-production and decay.

Pair-production of Z^0Z^0 is one of the most significant event, as each of the Z^0 can decay to a $l\bar{l}$ pair, that has the clearest signature in the ATLAS detector, as compared to WW or WZ pairs. The decay of the Z^0 boson to 2-leptons, either $e\bar{e}$, $\mu\bar{\mu}$ or $\tau\bar{\tau}$, only has a branching ratio of $\Gamma_{l\bar{l}}/\Gamma = 10.0970.003\%$, whereas a decay into hadrons, and therefore jets is of far higher probability ($\Gamma_{jets}/\Gamma = 69.910.06\%$), it is far easier to study. The remaining decay branch is $Z^0 \rightarrow e + \nu_e$. One could also use this branch for our study, but neutrinos are almost undetectable, at least by direct measurement.

Having then understood which decay process for the Z^0Z^0 pair decay we would like to use, one needs to proceed to accurately avoid the two other cases of decay mentioned above. The contributing decay products that give rise to either the lepton-neutrino or the hadronic jets case are the Z^0bb , that is, a Z^0 boson and a pair of bottom-anti-bottom quarks, and the case of having a top-anti-top quark $t\bar{t}$. One should then recall that our desired case is the pure production of 4-leptons case, with no other by-products.

We are provided then with a Monte Carlo simulation of decays of these branches, as well as a data-set of data from the ATLAS experiment. Initially one sets to the task of applying cuts to the three mentioned cases above: Z^0Z^0 , Z^0bb , $t\bar{t}$. On the real ATLAS data-set all possible decay branches are displayed, therefore our need to come up with the desired cuts, to ensure that after our cut-selection is applied, the real data will be mainly composed of $Z^0Z^0 \rightarrow l\bar{l}l\bar{l}$. In Fig. 19 one can see the initial Monte Carlo data-set, where we have the three decay branches. Take notice of the total count on top of each graph (Entries), that account for the total number of counts of each type. Applying three set of cuts, being:

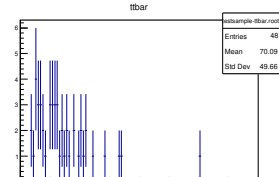
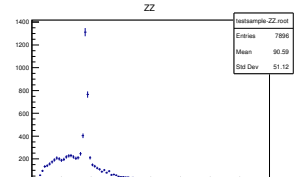
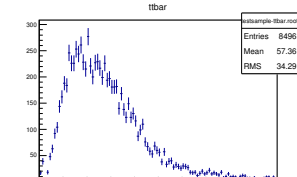
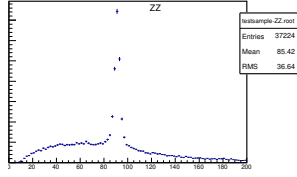


Figure 19: The ZZ Monte Carlo events without cuts.

Figure 20: After applying the cut

- Enforce that the final product be composed of two leptons and two anti-leptons. This ensures that the final state has the desired 4-leptons, but does not impede the existence of other particles, such as neutrinos;
- Enforce that there are no jets on the final states. One can see the considerable reduction effect on both the $t\bar{t}$ and $Z^0 b\bar{b}$ decay
- Lastly one enforces that all cases where there is any missing transverse energy $\cancel{E}_T > 16$ GeV are disregarded. This ensure the cases where one would have emission of neutrinos is not taking into account.

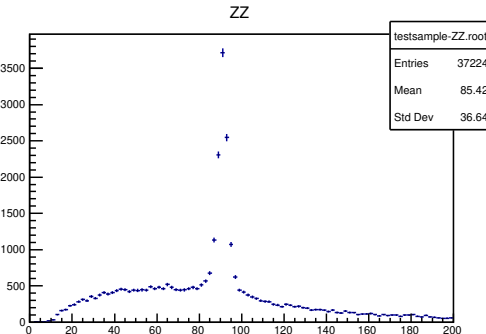
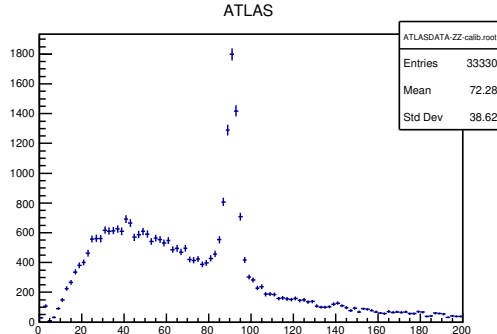


Figure 21: ATLAS data before applying the cuts

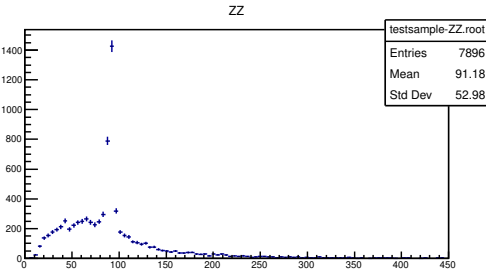
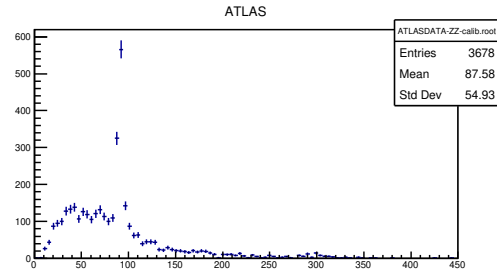


Figure 22: ATLAS data after applying the cuts

Having thus set a reasonable selection of cuts to the model data, the output is shown in Figure 20 then one applies the same cuts to the real ATLAS data-sets, which does include all branching decays, thus ensuring,

to a certain degree, that we are only analysing a 4-lepton final state. In Figure 21 and Figure 22 one can now see the real and simulated data, side-by-side, before and after the applied cut-selection.

8.2 The three types of decay: ZZ, ZZ* and Z*Z*

Furthermore, an overview study to distinguish real and virtual Z^0 bosons is put forward. Since all these bosons come from previous decays, they need not be on-shell. A quick overview of the energy spectrum of the 4-lepton invariant mass, of both data-sets, allows for a qualitative analysis of the overall count of Z^0Z^0 pair decays. In Figure 25, two real ZZ bosons decays give rise to a invariant mass of the 4-lepton case to have a well defined mass, peaking at $2M_Z - 2\Gamma_Z < 2M_{4l} < 2M_Z + 2\Gamma_Z$. The case of one real one virtual boson Z^*Z is bounded at a spectra of $M_{4l} > M_Z - \Gamma_Z$, that is, one real Z is created, but the virtual boson can have any mass which is shown in Figure 26. Lastly, the case of having two virtual bosons Z^*Z^* lead to an unbounded spectrum of energies. When we look back at Figure 27, one can associate the peak to mainly the ZZ decays, whereas the wide spectrum is associated to the two other cases of virtual particles.

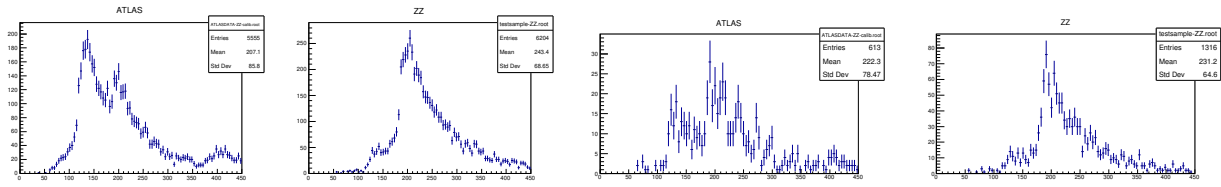


Figure 23: Invariant mass plot with cuts for all ZZ with no cuts

Figure 24: Invariant mass plot with cuts for all ZZ cases

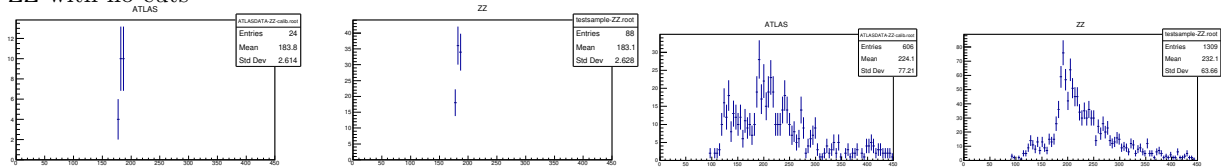


Figure 25: Invariant mass plot with cuts for both real ZZ boson decay

Figure 26: Invariant mass plot with cuts for One real Z and One Virtual Z

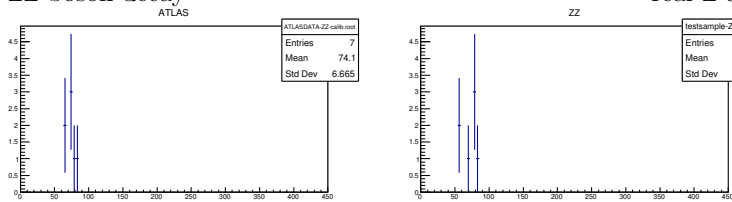


Figure 27: Invariant mass plot with cuts for both virtual ZZ

In conclusion, one has obtained a consistent overview and analysis of the Z^0Z^0 decay, restricted accordingly the cuts and studied the possibility of off-shell² decays. One can finally proceed to study the four cases of physics beyond the SM.

8.3 New Physics

Since the 4-lepton decay leaves the most distinct signature on the detector, we use precisely this type of decay to further study other exotic cases of physics beyond the SM. Our first case-study is the Higgs' mechanism

²off-shell particles are the virtual particles, when their mass is not equal to their rest mass while on-shell are the real particles where their masses is equal to the rest mass and follow the equation $E^2 = p^2 + m^2$

8.4 Higgs' Mechanism

The existence of the Higgs' boson of spin 0 can break the weak symmetry, giving mass to the weak gauge bosons, such as the Z^0 . One can thus have the case of $H \rightarrow ZZ^* \rightarrow l\bar{l}l\bar{l}$, as seen in Figure 5, one take a closer look at the 4-lepton invariant mass outside the peak area of the ZZ boson decay. A possible decay peak is found at $M_{4l} \approx 125 \pm 5\text{GeV}$. The counts are still low, but as expected, in any search for decays beyond the SM, such cross sections should be considerably small.

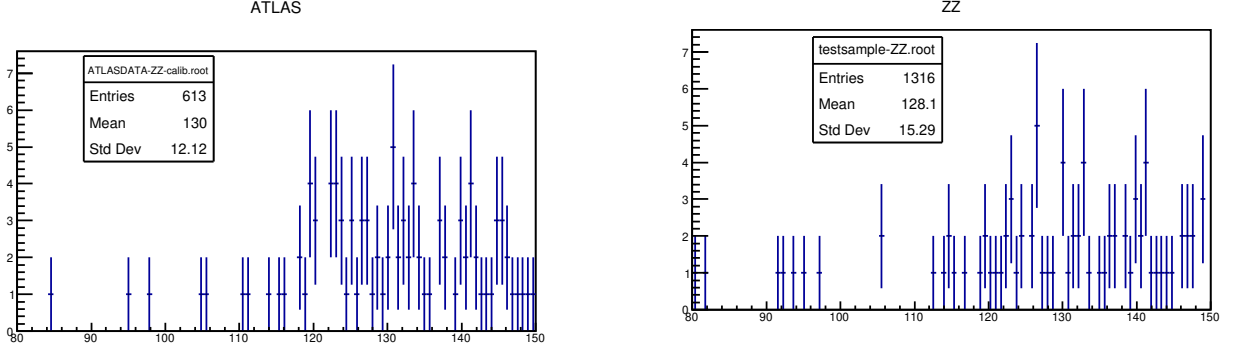


Figure 28: Invariant mass plot pd 4-leptons for the search of Higgs boson

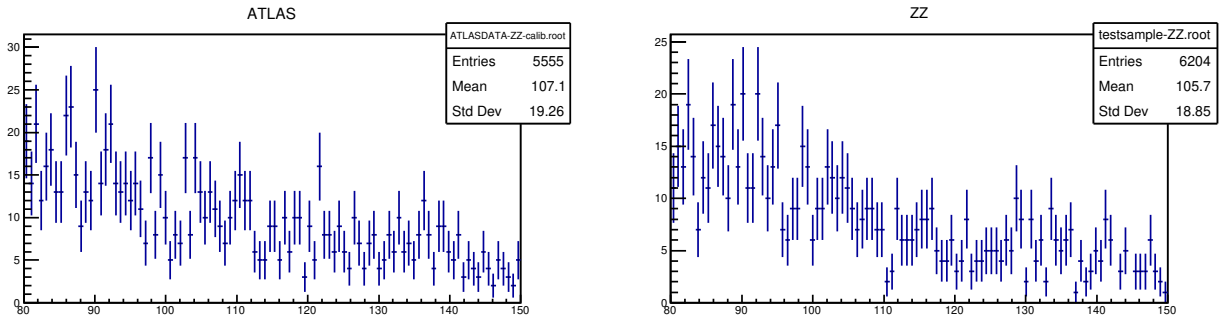


Figure 29: Higgs signal with the background events for the 4-leptons channel

The events for the Higgs signal is 613 (Figure 28) lower than the expected, Figure 29 and that of the background with Higgs signal (Figure 29) as 5555. The events number aren't excess and we cannot calculate the significance which is defined as $\frac{S}{\sqrt{B}}$. S is excess number of events than the expected.

8.5 Heavy Gauge Bosons Z^0

Another possibility put forward is the existence of weak gauge bosons Z^0 heavier than the two Standard model gauge bosons. One would expect them to be heavier than the one predicted in the SM, else they would have already been detected. Since in the case of the Higgs' mechanism one expected a possible peak around M_H , now we can look for the invariant mass plots of 2-lepton decay. Recall that we need to account for all possible combinations amongst the four leptons that are decaying. One takes special attention to peaks above the value of M_Z .

In Figure 30, one can find an interesting peak situated around $2M_{Z^0}$. The important comparison between this case and the previous with the Higgs' boson is the necessity of the existence of two peaks, equivalent to having a two real Z^0Z^0 decay or a one real one virtual Z^*Z decay, giving respectively peaks around $2M_{Z^0}$ and M_{Z^0} . In Figure 31, one can find a possible peak of a $M_{Z^0} \approx 280$ GeV. In panel a) one can distinguish the existence of this peak, but an argument against the existence of such boson is then put forward, since in panel c), depicting this time the 4-lepton invariant mass, one should see a peak at $2M_{Z^0} \approx 560\text{GeV}$ (Figure

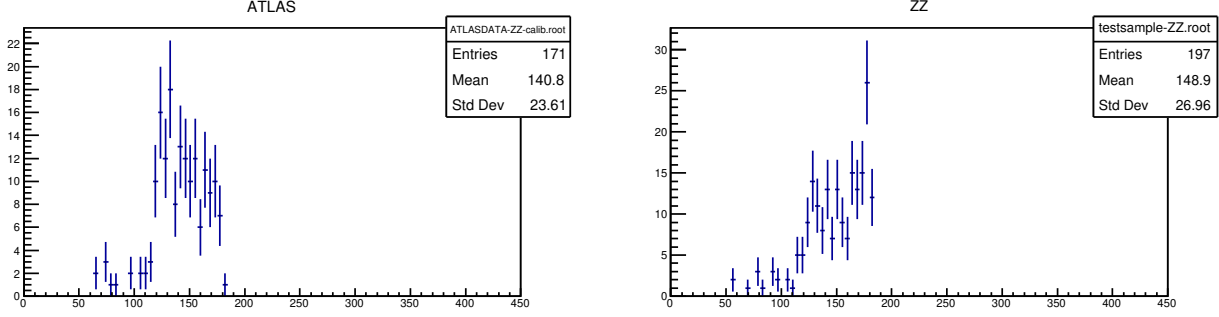


Figure 30: Invariant mass plot of the 2-leptons lower than 180 GeV

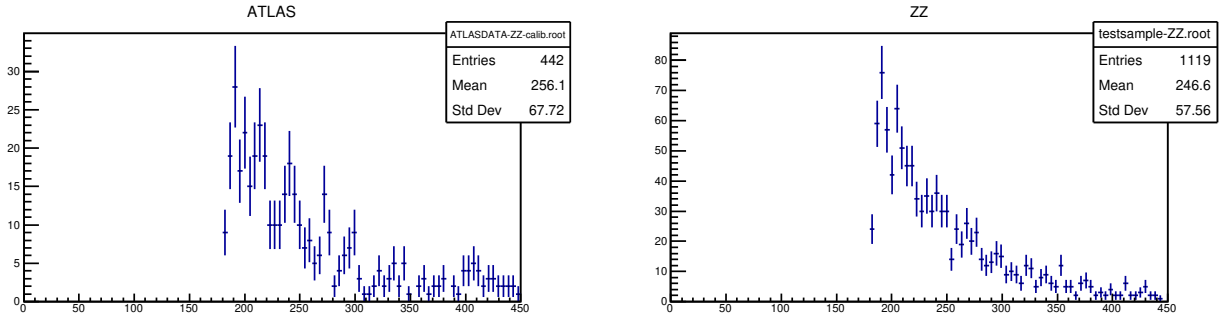


Figure 31: Invariant mass plot of the 2-leptons higher than 180 GeV

24). The nonexistence of this peak argues against the possibility of existence of a heavier gauge boson, such as the Z' boson.

8.6 Supersymmetry Model

Thirdly, one considers the possibility of an equivalent process arising from the SuSy model. According to the SuSy model, there exists a similar decay of a Z^0 pair, leading to a 4-lepton end state (Figure 6).

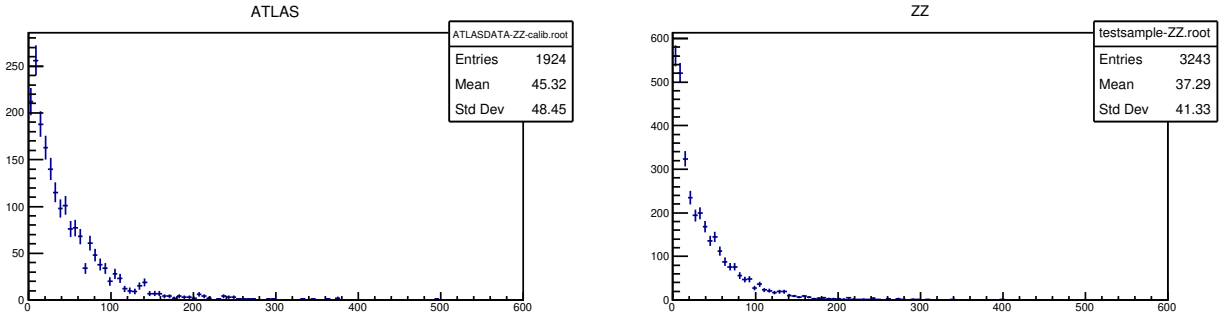


Figure 32: Missing transverse energy E_T

A consequence of this model is the existence of χ^0 particles, known as Lightest Supersymmetrical Particles, or LSP, and named neutralinos. They, alike the neutrinos, interact very dimly with the detector, and thus one has to try to indirectly measure them. One can therefore lift the previous applied cut on the $E_T < 16$, and further look for discrepancies between the ATLAS and the Monte Carlo data-set. In Figure 32, one can see the plot for the E_T of both datasets.

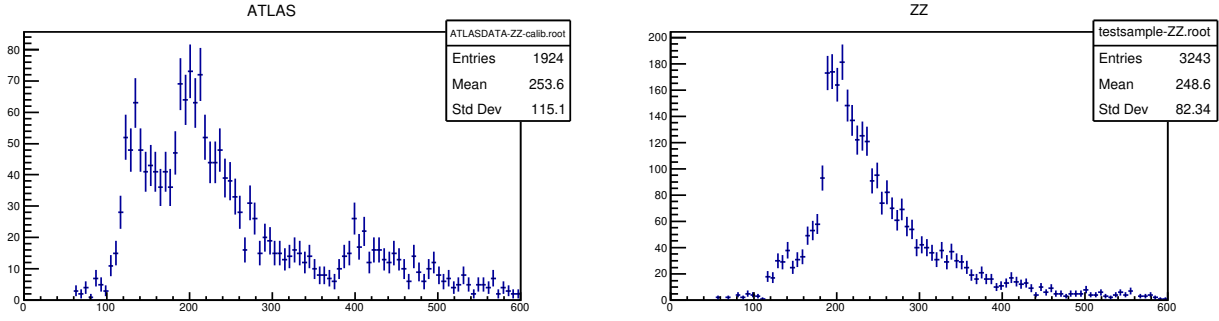


Figure 33: Invariant mass plot of 4-leptons for search of SUSY Particles

8.7 Fourth Generation quarks

Lastly, one analyses the possible case of the existence of heavier quarks. Equivalently to the Z^0 hypothesis, the quarks should have a bigger mass than the known quarks, else we could have probably already detected. This hypothesis also arises from the fact that the SM does not set a limit to the generation number of the fermions. We know about the existence of three generations, but there is nothing limiting the SM to have a fourth, or even higher, generation, of higher mass.

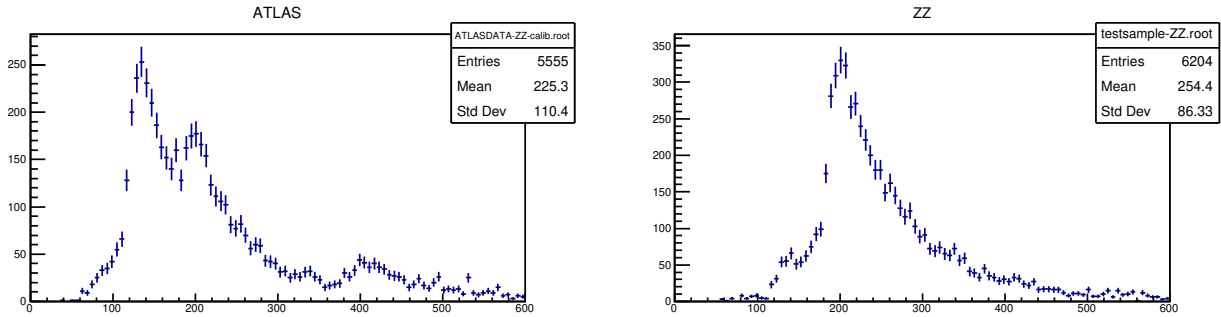


Figure 34: Invariant mass plot of 4-leptons for the search of heavy quarks

Consequently, one can work with for example with the d_4 quark, our hypothesis of a -1/3 charge quark of mass greater than the top quark t , so equivalent to the down quark d , but belonging to the fourth generation, hence d_4 . Such quark should have such a high mass, that alike the top quark, it would decay extremely fast to a lower mass quark, as the t quark, initiating a cascade process which is shown in Figure 7 and given as

$$gg \rightarrow d_4 \bar{d}_4 \rightarrow tW^- \bar{t}W^+ \rightarrow bW^- \bar{b}W^+ \rightarrow 2\text{or}4 \text{ leptons} + \text{neutrinos} + \text{jets} \quad (7)$$

Since this decay rather always gives rise to jets, as well as neutrinos, we proceed to lift our previous two cuts, and thus studying the cases where we have E_T as well as non-zero jets 7 . In Figure 34, one can see the plot of the invariant mass of the 4-leptons, whereas these plots account for both the possible neutrinos and existence of jets, just like desired. There seems to be no direct evidence of a distinguishable case between both data-sets.

9 Conclusion

The experiment was performed and various mentioned tasks were completed. The visual analysis of the events in the ATLANTIS software enabled us to learn how to visually identify particles observing their interactions and also get a quantitative idea of various measured quantities like energy and momentum of the particles. Further the detector was calibrated for invariant mass measurement as we might measure wrongly because of the various systematic errors. The detector was calibrated by taking a set of cuts of the

ATLAS detector. A calibration mass of the Z^0 bosons was attained at $M_{cal} = 91.140.02\text{GeV}$. The next part includes the analysis of the Z^0 decays and distinguishing real and virtual bosons. Various cuts were used for the same, however, no precise method could be given to distinguish a virtual decay mode because of its freedom to be as off -shell as it wants, greater or lesser than the range for real bosons. So we expect these modes to contain significant background.

The last revolved around finding examples of New Physics, including the investigation of four prospective cases afore mentioned. It was found that the invariant mass of the 4-leptons and the missing transverse energy ($\cancel{E_T}$) are the sensitive observables to the search of Higgs and new physics. The cases with 4-lepton end products were statistically analysed placing different cuts for different cases. It was concluded that the data has a possible evidence for the existence of Higgs boson at a possible invariant mass of $M_H = 125 \pm 5\text{GeV}$ with significance with no significance. All other cases showed no significant data. All throughout the experiment, the ROOT software was used for the analysis. The questions to be answered in the experiment manual are attached in the appendix.

10 Acknowledgement

We acknowledge the Bonn-Cologne Graduate School for the access to the equipments. We wish to thank Ph.D. Christian Nass for the tutoring and helpful insights that guided us successfully through the experiment.

References

- [1] Advanced Laboratory Course physics601 manual, E214, University of Bonn
- [2] Retrieved from: "<https://en.wikipedia.org/wiki/StandardModel>"
- [3] Retrieved from, "<https://en.wikipedia.org/wiki/Feynmandiagram>"
- [4] Retrieved from, "<http://boojum.as.arizona.edu/jill/NS1022006/Lectures/Cosmology/>"
- [5] Modern particle physics. Cambridge University Press Thomson, M. (2013).
- [6] N Khetan and L Rydin Gorjão, (2015) E214: Atlas. unpublished, Experimental report. Rheinische-Friedrich-Wilhelms University of Bonn
- [7] Retrieved from "<https://scitechdaily.com/as-supersymmetry-fails-physicists-looking-for-new-models/>"
- [8] Retrieved from "<https://home.cern/resources/faqs/facts-and-figures-about-lhc>"
- [9] Retrieved from "<https://en.wikipedia.org/wiki/CERN/media/File:Cern-accelerator-complex.svg>"
- [10] Retrieved from "<https://atlas.cern/discover/detector>"
- [11] Retrieved from "<https://slideplayer.com/slide/10416710/>"
- [12] Retrieved from: "<https://cerncourier.com/a/run-2-data-set-pins-down-higgs-boson-properties/>"

11 Appendix

Pre-lab Questions

1. Decay of a Z^0 Boson:

Which value does the momentum of an electron have in the decay of a Z^0 boson if the Z^0 is at rest?

$$Z^0 \rightarrow e^+ \quad e^-$$

Solution:

Let p_Z , p_{e^+} , and p_{e^-} be the four momenta vectors of Z^0 , e^+ and e^- respectively. Then using momentum conservation:

$$(p_Z)^2 = (p_{e^+} + p_{e^-})^2 = p_{e^+}^2 + p_{e^-}^2 + 2 \cdot p_{e^+} \cdot p_{e^-}$$

Then,

$$(m_Z)^2 = 2 \cdot m_e^2 + 2E_{e^+} \cdot E_{e^-} - 2\vec{p}_{e^+} \cdot \vec{p}_{e^-}$$

And since, $E_{e^+} = E_{e^-} \simeq E$

$$\vec{p}_{e^+} \cdot \vec{p}_{e^-} = |p_{e^+}| \cdot |p_{e^-}| \cos \theta, \text{ where } \theta = \pi$$

Neglecting the mass of electron, the energy-momentum relation then gives:

$$(E_e)^2 = m_e^2 + |\vec{p}_e|^2 \approx |\vec{p}_e|^2$$

Thus

$$(m_Z)^2 = 2 \cdot m_e^2 + 2E^2 + 2 \cdot |\vec{p}_{e^+}| \cdot |\vec{p}_{e^-}| \approx 4E^2 \implies |\vec{p}_e| \approx \sqrt{\frac{m_Z^2}{4}} = 45.595 \text{ GeV}$$

2. Scattering Reaction:

How large is the momentum of a tau lepton in the reaction;

$$e^+ \quad e^- \rightarrow \tau^+ \quad \tau^-$$

if the reaction takes place in the center-of-mass system, with a center-of-mass Energy 5GeV?

Solution:

In the centre of mass frame, $E_{CM}^{initial} = 5 \text{ GeV}$ is divided equally among the produced particles from symmetry and conservation laws. Thus

$$E_{\tau^+} = E_{\tau^-} = 2.5 \text{ GeV}$$

$$\implies |\vec{p}_{\tau^\pm}| = \sqrt{E_{\tau^\pm}^2 - m_{\tau^\pm}^2} = 1.75 \text{ GeV}$$

3.

What is the minimum invariant 4-lepton-mass, when the four leptons originate from a Z^0 pair? Why do you find 4-leptons-events with invariant mass beneath this threshold?

Solution:

In case of a real Z^0 pair, the minimum invariant mass of the produced 4-leptons would be $4 \times \frac{m_{Z^0}}{2} = 2M_{Z^0}$, in the center-of-mass frame. However, if one or both of the Z^0 particles is virtual, that would allow for invariant masses below this threshold.

4.

Consider a Higgs boson which decays into two Z^0 bosons. How does the distribution of the 4-lepton-invariant mass look like?

Solution:

The 4-lepton invariant mass curve shall follow a Breit-Wigner fashion peaking around the value of the Higgs boson as shown in Figure 35.

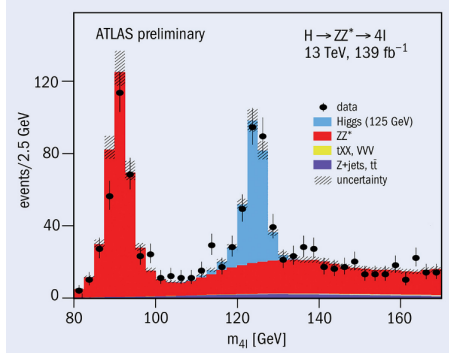


Figure 35: 4-lepton invariant mass curve[12]

5.

Assume you have an ideal detector. what is the typical \cancel{E}_T if a Z^0 pair has been produced and both Z^0 decay into electron or muon pairs? What \cancel{E}_T will you expect when you have a real detector?

Solution:

An ideal detector means a 100% efficiency in detecting the outcome of a scattering process and hence a 100% detection of the produces e^+e^- and $\mu^+\mu^-$ pairs that are the result of the Z^0 boson decay. So there will be no missing transverse momentum. On the other hand, a non-ideal, real detector would result in a loss and/or noise in the detection and will have a non-zero \cancel{E}_T .

6.

The Branching ratio of $t \rightarrow W b$ is almost 100%. If you have a top anti-top pair in an event, both particles decay instantly via $t \rightarrow bW$. If both W bosons each decay leptonically ($W \rightarrow l\nu$), one finds two leptons in the event. What could explain the occurrence of 4 leptons in a $t\bar{t}$ event?

Solution:

- The W boson would decay into a lepton and a neutrino.
- The bottom quark would undergo hadronization creating B-mesons.
- The B-mesons undergoes semi-leptonic decay into leptons and neutrinos.

The produced leptons thus far result in a 4 leptons in a $t\bar{t}$ event. It is shown in Figure 36.

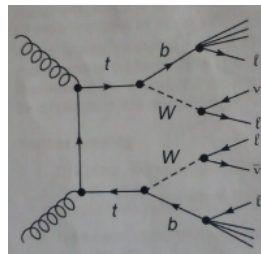


Figure 36: 4-lepton $t\bar{t}$ Events[1]

7. Gedanken-Experiment:

Create a random integer number between 1 and 200. You record the occurrence of each integer in a histogram with 200 bins. After histogramming 20,000 numbers you expect on average 100 entries per bin.

- (a) What is the statistical error for the number of entries in one bin?

Solution:

The statistical error associated with each bin would scale as \sqrt{N} with N being the number of entries in each bin. Hence here,

$$N = 100 \implies \sqrt{N} = 10$$

- (b) What is the probability of finding a bin with 130 entries?

Solution:

A bin with 130 entries is 30 entries away from the mean bin size 100. Since $\sigma = 10$, such a bin would be 3σ away from the mean, and hence merely 0.3% probable.

- (c) How many of such 130 entry bins (in average) do you expect to appear in 200 bins?

Solution:

This would be 0.3% of 200 \implies 0.6 bins.